P1.6 LIGHTNING SIGNATURES OF LONG-LIVED TORNADIC SUPERCELLS IN THE SOUTHEASTERN U.S. ON 27-28 APRIL 2011

Stephen M. Strader* and Walker S. Ashley
Meteorology Program, Department of Geography, Northern Illinois University, De Kalb, IL

1. Introduction

Since the installation of the National Lightning Detection Network (NLDN) in the late 1980s, remotely sensed lightning attributes have been employed as useful nowcasting tools for convection (Kufa and Snow 2006; Cope 2006). Most notably, lightning characteristics and patterns associated with supercells, including those capable of producing tornadoes, have been examined extensively using a multitude of research techniques. These methods include: relating updraft strengthening (weakening) to the production of convective hazards that include tornadoes, large hail, and downbursts (Murphy *et al.* 2005; McKinney *et al.* 2008); analyzing a supercell's charge structure and the surrounding environment's role on modifying a supercell's charge structure (Smith *et al.* 2000); and the assessment of total cloud-to-ground (CG) lightning flash rates in relation to the timing of tornadogenesis (Seimon *et al.* 1993; MacGorman *et al.* 1994; Knapp *et al.* 1994; Perez *et al.* 1997; Bluestein *et al.* 1998; McCaul *et al.* 2002; Knupp and Paech *et al.* 2003; Carey *et al.* 2003; McDonald *et al.* 2006).

This study integrates past research methodologies to analyze the lightning and severe weather hazard relationship for the 27-28 April 2011 Southeast U.S. tornado outbreak. Lightning data from the NLDN are employed to examine the lightning characteristics associated with seven supercell thunderstorms that produced long-track, significant and/or violent tornadoes.

*Corresponding author address: Stephen M. Strader, Northern Illinois University, Department of Geography, Meteorology Program, De Kalb, IL 60115; sstrader@niu.edu

2. Data and Methodology

For this investigation, seven long-lived tornadic (EF-3 or greater and damage paths of 32 km or longer) supercells that occurred during the timeframe of 12 UTC 27 April 2011 to 12 UTC 28 April 2011 are examined using the NLDN and the National Climatic Data Center (NCDC) Doppler radar archive (Table 1; Figure 1). Employing both spatiotemporal and statistical methodologies, this study presents a comprehensive and relatively controlled examination of the total CG lightning flash-tornado relationship of long-lived tornadic supercells that developed, matured, and evolved in a similar kinematic and thermodynamic environment (i.e., low-level moisture values, storm relative helicity, convective available potential energy, etc.). While prior research has examined the lightning-tornado relationship (Kane 1991; Seimon 1993; Knapp 1994; MacGorman and Burgess 1994; Perez *et al.* 1997; Bluestein *et al.* 1998; McCaul *et al.* 2002; Carey *et al.* 2003; Knupp and Paech *et al.* 2003; Martinez and Schroeder 2004; McDonald and McCarthy 2006; McKinney *et al.* 2009), this study is the first to analyze the lightning-tornado relationship for such an extreme severe weather outbreak Moreover, similar to past studies, this research contends that CG lightning flash rates, in conjunction with radar observations and other forms of mesoanalysis, can be used to understand better severe thunderstorm dynamics and evolution (MacGorman *et al.* 1989; Carey and Rutledge 1998; Harlin *et al.* 2000; MacGorman *et al.* 2002; Lang and Rutledge 2002; Stieger *et al.* 2005; and Kufa and Snow 2006).

The NLDN data contains location (latitude and longitude) of lightning flash (cloud or ground), time (milliseconds), peak flash polarity (+ or -), amplitude (kiloamp (kA)), multiplicity, and error ellipse values (km) for each lightning flash. The

NLDN has a self-reported lightning detection efficiency of 99%, a flash detection efficiency of 95%, and a median location accuracy of 250-500 meters (Vaisala 2011).

Temporal analyses were conducted throughout the life cycle of each of the seven storms in the study. The temporal analyses illustrate total CG lightning flashes (both positive and negative polarities), total positive cloud-to-ground (+CG) lightning flashes, total negative cloud-to-ground (-CG) lightning flashes, time of tornadogenesis, duration of tornado, maximum tornado damage rating using the enhanced Fujita scale, and time of tornadolysis. This permitted statistical analyses of percent difference, count, CG lightning flash rates, and measures of central tendency (mean), which were used to evaluate each storm in comparison to the others. These temporal analyses were used to determine whether or not a local maximum prior to tornadogensis, local minimum coincident with tornado touchdown, an increase in total CG lightning flash rate coincident with tornadolysis, and/or a polarity shift occurred coincident with tornado touchdown or during tornado production occurred in each storm. Further, temporal analyses were used to examine the total CG lightning flash rate and low-level mesocyclone (measured from lowest elevation scan altitude to 4 km or, effectively, 0-4 km AGL) relationship. Rotational velocity (V_r) and azimuthal (rotational) shear (S) were calculated and utilized to determine the strength of the low-level mesocyclone. Similar to Stumpf *et al.* (1998), Atkins *et al.* (2005), and Wolf (2006), rotational velocity was defined as $(V_{max} – V_{min})/2$ where V_{max} and V_{min} are the outbound and inbound storm-relative velocities, respectively. Also, similar to the methods of Stumpf *et al.* (1998), azimuthal (rotational) shear (S) was defined as V_r / D where D is the distance between V_{max} and V_{min}. Due to Doppler radar coverage issues, some storms within the research domain were excluded from this dataset. This was primarily due to the radar beam's inability to sample the lowest four km of the storm, precluding information on the strength of the low-level mesocyclone.

3. Results

a. Regional Analysis

Regional analysis indicates that there were 109,206 total CG lightning flashes for the 300 km regional buffer centered on Birmingham, AL for the time period of 19 UTC 27 April 27 2011 through 02 UTC April 28 2011 (Table 2). Additionally, 5.39% of the total CG lightning flashes recorded were +CG lightning flashes. This percentage is consistent with prior results found in Orville *et al.* (2010) where the annual and spatial variation in +CG flash percentage varied from 2% in the Southeastern U.S. (i.e. Florida) to 25% along the western coast of Alaska. Specifically for the seven supercells analyzed, there were 38,445 total CG lightning flashes produced by these storms, constituting 6.57% +CG flashes and 93.42% -CG flashes (Table 3).

b. Individual Storm Analysis

All storms examined within this study experienced average total CG lightning flash rates greater than 11 flashes min^{-1} throughout their life cycles (Table 4). In comparison to tornadic storms in Perez *et al.* (1997) — where the average total CG lightning flash rate for all storms that produced a tornado with a path length of 32 km (20 miles) or greater was 4.19 flashes min^{-1} — the average total CG lightning flash rate for supercells examined in this study was a much higher 27.97 flashes min^{-1}. In addition, the percentage +CG lightning flashes was 7.45% for the storms assessed, which is much lower than the 22.87% found in Perez *et al.* (1997). However, it is likely that the 27-28 April 2011 storms produced a lower percentage +CG lightning flashes because of the spatiotemporal characteristics of the severe weather event. Previous lightning climatology research (Makela *et al.* 2010; Orville *et al.* 2010) suggest that the geographic location and season of occurrence of this particular event may be the reason +CG lightning flashes were less common. Moreover, storms dominated by +CG flashes tend to occur in environments with drier low to mid-level tropospheric air (i.e., low dew points, low mean-mixing ratios in the lowest 100 kPa of the troposphere, higher lifted condensation levels

(LCL), low precipitable water (PW) values from the surface to 400 kPa, etc.; Carey and Buffalo 2007). Drier atmospheric conditions ultimately lead to broader updrafts that result in greater updraft velocities, greater collision velocities, and less entrainment of dry air. Thus, the combination of these relatively dry atmospheric variables result in reversed-polarity charging in the mixed phase region of the storm (Carey and Buffalo 2007). The storms that occurred on 27 April 2011 contained high dew point temperatures, high PW values, and low LCL heights, which is suggestive of why the storms were dominated by negative polarity lightning flashes. In addition, the very low LCL heights that characterized this event were indicative of the potential for a larger warm cloud depth (WCD), which has been found to increase the efficiency of warm rain-collision-coalescence processes (Rosenfeld and Woodley 2003; Carey and Buffalo 2007). This efficiency enhancement would, in turn, result in a much greater percentage of -CG flashes in comparison to +CG flashes. Overall, it appears that the supercells that occurred on 27-28 April 2011 were not only efficient producers of long-lived, long-tracked, violent tornadoes, but also produced greater CG lightning flash rates in comparison to typical long-lived supercell examined in prior research (Perez *et al.* 1997).

Of the seven supercells examined, Storm B was the most prolific in terms of average total CG lightning flashes min^{-1}, exemplifying an average total CG lightning flash rate of 59.65 flashes min^{-1} (Table 4). We speculate that the reason Storm B constituted the greatest average total lightning flash rate was because of its high liquid water, ice, and graupel content as well as ice particle seeding from the anvil of an upstream storm (Storm A; Brooks and Doswell 1994; Saunders 1994; MacGorman and Burgess 1994; Knupp *et al.* 2003). Storm F produced the lowest average total CG flash rate; in this case, the average total CG flash rate was 11.16 flashes min^{-1} (Table 4).

c. Lightning and Tornado Relationship

The majority of supercells (6 of the 7) examined experienced a local maximum in total CG lightning flash rate prior to tornadogenesis and a local minimum in total CG lightning flash rate coincident with tornadogenesis (Table 5; Figures 2 through 8). A local maximum in total CG lightning flash rate was defined as a total CG lightning flash rate of change greater than 0.5 flashes min^{-1} in the fifteen minutes prior to tornadogenesis; whereas, a local minimum in total CG lightning flash rate coincident with tornadogenesis was defined as a negative rate of change of -0.5 flashes min^{-1} or greater in the five-minutes prior to tornadogenesis or during the five-minute lightning data bin that encompassed the time of touchdown. An increase in total CG lightning flash rate coincident with tornadolysis was defined as a rate of change in total CG lightning flash rate greater than 0.5 flashes min^{-1} in the five minutes prior to tornado dissipation or during the five-minute lightning data bin that encompassed the time of tornado dissipation. Storms C, D, F, and G all experienced a local maximum in total CG lightning flash rate prior to tornadogenesis, a local minimum in total CG lightning flash rate coincident with tornadogenesis, and an increase in total CG lightning flash rate coincident with tornadolysis at least once throughout their life cycles (Table 5; Figures 4 and 5; Figures 7 and 8).

Of those storms that experienced a local maximum in total CG lightning flash rate, Storm G exemplifies the greatest rate of change for a local maximum prior to tornadogenesis (19 flashes $min^{-1;}$ Figure 8). Storm C (tornado C-2) had the lowest rate of change for the local maximum prior to tornadogenesis with 4.4 flashes min^{-1} (Figure 4). In comparison to all other tornadoes within this study, tornado D-1 exemplifies the greatest rate of change for total CG lightning flash rate coincident with tornadogenesis (-10.4 flashes min^{-1}; Figure 5). Conversely, tornado C-1 experienced the lowest rate of change in total CG lightning flash rate coincident with tornadogenesis (-1.2 flashes min^{-1}; Figure 4). Additionally, tornado C-4 and D-1 represent the greatest rates of change for total CG lightning flashes that exemplify an increase in total CG lightning flash rate at tornadolysis (Figure 4).

The findings from this study support prior research (Perez *et al.* 1997; Bluestein *et al.* 1998;

Lang and Rutledge 2005; McDonald and McCarthy 2006; McKinney *et al.* 2009) that suggest an increase in total CG lightning flash rates typically occurs in the moments prior to tornadogenesis. Additionally, results corroborate prior research (Seimon 1993; Knapp 1994; Perez *et al.* 1997; McDonald and McCarthy 2006) that indicate tornadogenesis tends to occur during times of decreased or minimum total CG lightning flashes.

Contrary to the results in Perez *et al.* (1997) and Martinez and Schroeder (2004), none of the storms presented in this study experienced a polarity shift that occurred prior to tornadogenesis, simultaneously with tornadogenesis, or during tornado production (Table 5). The lack of storms experiencing a polarity shift may be attributable to the time of year and location of the of the severe weather event (e.g. early spring, southeastern U.S.) when and where +CG lightning flashes are less common than the more frequently experienced -CG lightning flashes (Makela *et al.* 2010, Orville *et al.* 2010).

Overall, the majority of storms examined exhibit consistency with their total CG lightning flash rate and tornado relationship trends (Table 5); this is likely attributable to the fact that the storms formed in a similar kinematic and thermodynamic environment. These results follow that of Stieger *et al.* (2005) and Kufa and Snow (2006) who suggested that, although the variable nature of severe convective storms makes it difficult to utilize lightning flash trends for the nowcasting of severe-hazardous events, lightning flash trends could possibly be used for the nowcasting of hazards associated with thunderstorms given a similar kinematic and thermodynamic environment.

d. Lighting and Low-level Mesocyclone Intensity

Results from the low-level mesocyclone and total CG lightning flash rate analyses were diverse and variable among the four storms evaluated in the research domain (A, C, D, E). As in MacGorman *et al.* (1989), it was expected that, as the low-level mesocyclone strengthened, the two main charge regions within the supercell would be brought closer together and the majority of total lightning flashes would be cloud-to-air (CA), intra-cloud (IC), or cloud-to-cloud (CC) while CG lightning flash rates would decrease. However, results from this study suggest that the low-level mesocyclone and total CG lightning flash relationship is inconsistent.

Statistical tests (i.e., Pearson's product-moment correlation coefficient, significance testing with the t-distribution to determine whether or not the correlation coefficients (r) were statistically significant, and regression analysis) were applied to examine the relationship between azimuthal (rotational) shear total CG lightning flash rates. Correlation coefficient values of -1.0 to -0.5 are argued to be of *high* strength, -0.5 to -0.3 of *moderate* strength, and -0.3 to -0.1 of *weak* strength. Further, correlation coefficient values greater than -0.1 is indicative of *little to no* relationship between the two variables examined. All storms examined (A, C, D, E) were expected to have an inverse relationship (r value equal to -1.0 to -0.01) between rotational velocity or azimuthal shear and total CG lightning flash rate.

Overall, results on the low-level mesocyclone and total CG lightning flash rate relationship were varied and inconsistent among the storms examined. Storm A illustrated an inverse relationship of moderate strength between azimuthal shear and total CG lightning flash rate, Storm D (tornado D-2) had an inverse relationship of moderate to high strength between rotational velocity and total CG flash rate and Storm E had an inverse relationship of moderate strength between azimuthal shear (0.9 degrees elevation angle) and total CG flash rate (Tables 6 and 7; Figures 9 through 12). Storm C did not illustrate a statistically significant relationship between rotational velocity or azimuthal shear and total CG lightning flash rate using the one-tailed t-test (Table 8: Figures 13 and 14). The results found in this investigation suggest that the intensification or weakening of the low-level mesocyclone is one of many dynamical processes that influence a supercell's internal charge structure that ultimately affect the overall lightning production within the

storm (Stolzenburg *et al.* 1998; MacGorman *et al.* 2005; Wiens *et al.* 2005; Bruning *et al.* 2010).

4. Summary and Discussion

This study examined the lightning-tornado relationship for the 27-28 April 2011 Southeastern U.S. tornado outbreak. While past research has explored the lightning and severe weather hazard relationship, no investigation has observed the lightning-tornado relationship for such an unprecedented severe weather event. Additionally, this research analyzed the lightning characteristics of multiple, long-lived, tornadic supercells that formed in a similar kinematic and thermodynamic environment.

Results on the lightning-tornado relationship demonstrate that the majority of storms assessed exemplified a local maximum in total CG lightning flash rate prior to a local minimum in total CG lightning flash rate that was coincident with tornadogenesis (Table 11). Moreover, the majority of storms had an increase in total CG lightning flash rate concurrent with tornadolysis (Table 11). This distinctive lightning frequency pattern found during tornadogenesis (tornadolysis) was initially attributed to updraft intensification (weakening). However, examining the low-level mesocyclone intensity in relation to total CG lightning flash rate led to inconsistent results, which suggests that that low-level mesocyclone strengthening (weakening) is only one of many potential dynamical processes (e.g., precipitation development within the supercell updraft and downdraft regions, hydrometeor type, hydrometeor fall speeds, potential influence of lofted debris, etc.) that influence a storm's internal charge structure and subsequent CG lightning flash rates (Goodman *et al.* 1988; Williams *et al.* 1991; Bringi *et al.* 1997; Gilmore and Wicker 2002; Weins *et al.* 2005). Nevertheless, findings on the lightning-tornado relationship corroborate prior research that suggest an increase in total CG lightning flash rates typically occurs in the moments prior to tornadogenesis and tornadogenesis tended to occur during times of decreased or minimum CG lightning flashes (Perez *et al.* 1997; Bluestein et al. 1998; Lang and Rutledge 2005; McDonald and McCarthy 2006; McKinney *et al.* 2009; Seimon 1993; Knapp 1994; Perez *et al.* 1997; McDonald and McCarthy 2006). Further, the results support those found in McDonald and McCarthy (2006) where it was documented that total CG lightning flash rate increased as the tornado dissipated. As with Steiger *et al.* (2005) and Kufa and Snow (2006), we conclude that lightning flash trends can be used to assist in the nowcasting of hazards associated with severe storms.

Acknowledgements

Many thanks to Drs. Mace Bentley, Dave Changnon, and Andrew Krmenec who provided helpful comments, suggestions, and guidance throughout the entire research process.

References

Atkins, N. T., C. S. Bouchard, R. W. Przybylinski, R. J. Trapp, G. Schmocker, 2005: Damaging Surface Wind Mechanisms within the 10 June 2003 Saint Louis Bow Echo during BAMEX. *Mon. Wea. Rev.*, 133, 2275–2296.

Bluestein, H. B., and D. R. MacGorman, 1998: Evolution of Cloud-to-Ground Lightning Characteristics and Storm Structure in the Spearman, Texas, Tornadic Supercells of 31 May 1990. *Mon. Wea. Rev.,* 126, 1451-1467.

Bringi, V. N., K. R. Knupp, A. Detwiler, L. Liu, I. J. Caylor, R. A. Black, 1997: Evolution of a Florida thunderstorm during the Convection and Precipitation/Electrification Experiment: The case of 9 August 1991. *Mon. Wea. Rev.,* 125, 2131–2160.

Brooks, H. E., and C. A. Doswell III., Wilhelmson, R. B., 1994: The Role of Midtropospheric Winds in the Evolution and Maintenance of Low-Level Mesocyclones. *Mon. Wea. Rev.*, 122, 126-136.

Carey, L. D., K. M. Buffalo, 2007: Environmental Control of Cloud-to-Ground Lightning Polarity in Severe Storms. *Mon. Wea. Rev.*, 135, 1327-1353.

____, W. A. Petersen, R. A. Rutledge, 2003: Evolution of Cloud-to-Ground Lightning and Storm Structure in the Spencer, South Dakota Tornadic Supercell 30 May 1998. *Mon. Wea. Rev.*, 131, 1811-1831.

____, and S. A. Rutledge, 1998: Electrical and Multiparameter Radar Observations of a Severe Hailstorm. *J. Geophys. Res.*, 103, 13979-14000.

Cope, A. M., 2006: Toward Better Use of Lightning Data in Operational Forecasting, Preprints, 2nd Conf. on Meteorological Applications of Lightning Data, Atlanta, GA.

Gilmore, M.S., and L. J. Wicker, 2002: Influences of the Local Environment on Supercell Cloud-to-ground Lightning, Radar Characteristics, and Severe Weather on 2 June 1995. *Mon. Wea. Rev.* 130, 2349-2372.

Goodman, S. J., D. E. Buechler, P. D. Wright, W. D. Rust, 1988: Lightning and Precipitation History of a Microburst-producing Storm. *Geophys. Res. Lett.,* 15, 1185–1188.

Harlin, J. D., T. D. Hamlin, P. R. Krehbiel, R. J. Thomas, W. Rison, D. Shown, 2000: LMA Observations of Tornadic Storms During STEPS 2000. *Eos Trans. AGU*, 81, Fall Meet. Suppl., Abstract A52C-25.

Kane, R. J., 1991: Correlating Lightning to Severe Local Storms in the Northeastern United States. *Wea. Forecasting,* 6, 3–12.

Knapp, D. I., 1994: Using Cloud-to-Ground Lightning Data to Identify Tornadic Thunderstorm Signatures and Nowcast Severe Weather. *National Wea. Digest*. 19, 35-42.

Knupp, K. R., S. Paech, S. Goodman, 2003: Variations in Cloud-to-Ground Lightning Characteristics among Three Adjacent Tornadic Supercell Storms over the Tennessee Valley Region, *Mon. Wea. Rev.,* 131, 172-188.

Kufa, N., and R. Snow, 2006: Lightning: Meteorology's New Tool. Preprints, 2nd Conf. on Meteorological Applications of Lightning Data, Atlanta, GA.

Lang, T. J., and S. Rutledge, 2005: One Severe Storm with Two Distinct Electrical Regimes During its Lifetime: Implications for Nowcasting Severe Weather with Lightning Data. Preprints, *1st Conf. of Meteorological applications of Lightning Data,* San Diego, CA.

Lang, T. J., and S. A. Rutledge, 2006: Cloud-to-ground lightning downwind of the 2002 Hayman forest fire in Colorado. *Geophys. Res. Lett.*, 33, L03804, doi:10.1029/2005GL024608.

MacGorman, D. R., W. D. Rust, P. R. Krehbiel, W. Rison, E. C. Bruning, and K. Wiens, 2005: The Electrical Structure of Two Supercell Storms During STEPS. *Mon. Wea. Rev*., 133, 2583–2607.

____, and D. W. Burgess, 1994: Positive Cloud-to-Ground Lightning In Tornadic Storms and Hailstorms, *Mon. Wea. Rev*., 122, 1671-1697.

____, D. W. Burgess, V. Mazur, W. D. Rust, W. L. Taylor, and B. C. Johnson, 1989: Lightning Rates Relative to Tornadic Storm Evolution on 22 May 1981. *J. Atmos. Sci.*, 46, 221-250.

Makela, A., R., D. M. Pekka, D. Shultz, 2010: The Daily Cloud-to-Ground Lightning Flash Density in the Contiguous U. S. and Finland. *Mon. Wea. Rev.* DOI: 10.1175/2010MWR3517.1.

Martinez, M., and J. L. Schroder, 2004: Lightning Signatures in Convective Systems in the High Plains, Preprints, *22nd conf. on severe and local storms,* Hyannis, MA.

McCaul, E. W. Jr., D. E. Buechler, S. Hodanish, S. J. Goodman, 2002: The Almena, Kansas, Tornadic Storm of 3 June 1999: A Long-Lived Supercell with Very Little Cloud-to-Ground Lightning. *Mon. Wea. Rev*., 130, 407-415.

McDonald, M., P. J. McCarthy, D. Patrick, 2006: Anomalous Lightning Behavior In Northern Plains Tornadic Supercell. Preprints, *23rd conf. for Severe and Local Storms,* St. Louis, MO.

McKinney, C. M., L. D. Carey, G. R. Patrick, 2009: Total Lightning Observations of Supercells Over North Central Texas. *Electronic J. Severe Storms Meteor.*, 4 (2), 1–25.

Murphy, M. J., and N. W. Demetriades, 2005: An Analysis of Lightning Holes In a DFW Supercell Storm Using Total Lightning and Radar Information. Preprints, 85th Annual AMS meeting 2.3 Conf., San Diego, CA

Orville, R. E., Huffines, G. R., W. R. Burrows, K. L. Cummins, 2010: The North America Lightning Detection Network (NADLN): Analysis of Flash Data 2001-2009. *American Meteorological Society*. DOI: 10.1175/2010MWR3452.1.

Perez, A. H., L. J. Wicker, R. E. Orville, 1997: Characteristics of Cloud-to-Ground Lightning Associated with Violent Tornadoes. *Wea. Forecasting*, 12, 428-437.

Rosenfeld, D., and W. L. Woodley, 2003: Closing the 5-year Circle: From Cloud Seeding to Space and Back to Climate Change through Precipitation Physics. Cloud Systems, Hurricanes, and the Tropical Rainfall Measuring Mission (TRMM), Meteor. Monogr., No. 51, Amer. Meteor. Soc., 59–80.

Rudlosky, Scott D., Henry E. Fuelberg, 2011: Seasonal, Regional, and Storm-Scale Variability of Cloud-to-Ground Lightning Characteristics in Florida. *Mon. Wea. Rev*., 139, 1826–1843.

Saunders, C. P. R., 1994: Thunderstorm Electrification Laboratory Experiments and Charging Mechanisms. *J. Geophys. Res.,* 99, 10,773-10,779.

Seimon, A., 1993: Anomalous Cloud-to-Ground Lightning in an F-5- Tornado Producing Thunderstorm on 28 August 1990. *Bull. Amer. Meteor. Soc*., 74, 189-203.

Smith, S. B., J. G. LaDue, D. R. MacGorman, 2000: The Relationship Between Cloud-to-Ground Lightning Polarity and Surface Equivalent Potential Temperature During Three Tornadic Outbreaks. *Mon. Wea. Rev.,* 128, 3320-3328.

Steiger, S. M., R. E. Orville, M. J. Murphy, N. W. S. Demetriades, 2005: Total Lightning and Radar Characteristics of Supercells: Insights On Electrification and Severe Weather Forecasting. Preprints, *85th Annual AMS meeting 2.3 Conf.,* San Diego, CA.

Stolzenburg, M., W. D. Rust, T. C. Marshall, 1998: Electrical Structure in Thunderstorm Convective Regions. 3. Synthesis. *J. Geophys. Res.,* 103 (D12), 14,097-14,108.

Stumpf, G. J., A. E. Witt, M. DeWayne, S. L. Phillip, J. T. Johnson, M. D. Eilts, K.W. Thomas, D. W. Burgess, 1998: The National Severe Storms Laboratory Mesocyclone Detection Algorithm for the WSR-88D. *Wea. Forecasting*, 13, 304-326.

Vaisala Inc., cited 2011: National Lightning Detection Network. [Available online at http://www.vaisala.com/en/products/thunderstormandlightningdetectionsystems/Pages/NLDN.aspx.]

Weins, K. C., S. A. Rutledge, S. A. Tessendorf, 2005: The 29 June 2000 Supercell Observed during STEPS. Part II: Lightning and Charge Structure. *J. Atmos. Sci.*, 62, 4151–4177.

Williams, E. R., R. Zhang, and J. Rydock, 1991: Mixed-phase Microphysics and Cloud Electrification. *J. Atmos. Sci.*, 48, 2195–2203.

Wolf, R. 2006: A Preliminary Assessment of the Environmental and Radar Characteristics of Tornadic and Non-tornadic Mesovortices Associated with QLCSs. Preprints, *23rd Conf. Severe Local Storms*. St. Louis, MO

Table 1: Summary of the NWS survey results for tornadoes produced by the seven supercells examined in this study.

Storm	Number of tornadoes	Tornado location	Tornado	Peak damage rating	Fatalities	Path length (km)
A	1	*Mississippi*- Smithville; Chickasaw county *Alabama*-Shottsville	A-1	EF-5	29	111.7
B	1	*Alabama*- Hackleburg,; Franklin, Lawrence. Morgan, Limestone, Madison counties	B-1	EF-5	59	212.5
C	4	*Mississippi*- Neshoba, Kemper, Winston, Noxubee counties	C-1	EF-5	3	46.7
		Alabama- Cordova; Pickens, Tuscaloosa, Fayette, Walker, Blount counties	C-2	EF-4	13	187.4
		Alabama- DeKalb county	C-3	EF-5	N/A	54.4
		Georgia- Catoosa county *Tennessee*- Hamilton county	C-4	EF-4	20	80.5
D	2	Tuscaloosa, AL Birmingham, AL	D-1	EF-4	63	129.84
		Alabama- Jefferson, St. Clair, Calhoun, Etowah, Cherokee counties	D-2	EF-4	22	114.7
E	1	*Alabama*- Greene, Hale, Bibb Counties	E-1	EF-3	7	116
F	1	*Mississippi*- Smith, Jasper, Clarke counties *Alabama*- Choctaw county	F-1	EF-4	7	148.5
G	1	*Alabama*- Elmore, Tallapoosa, Chambers counties	G-1	EF-4	7	71.1

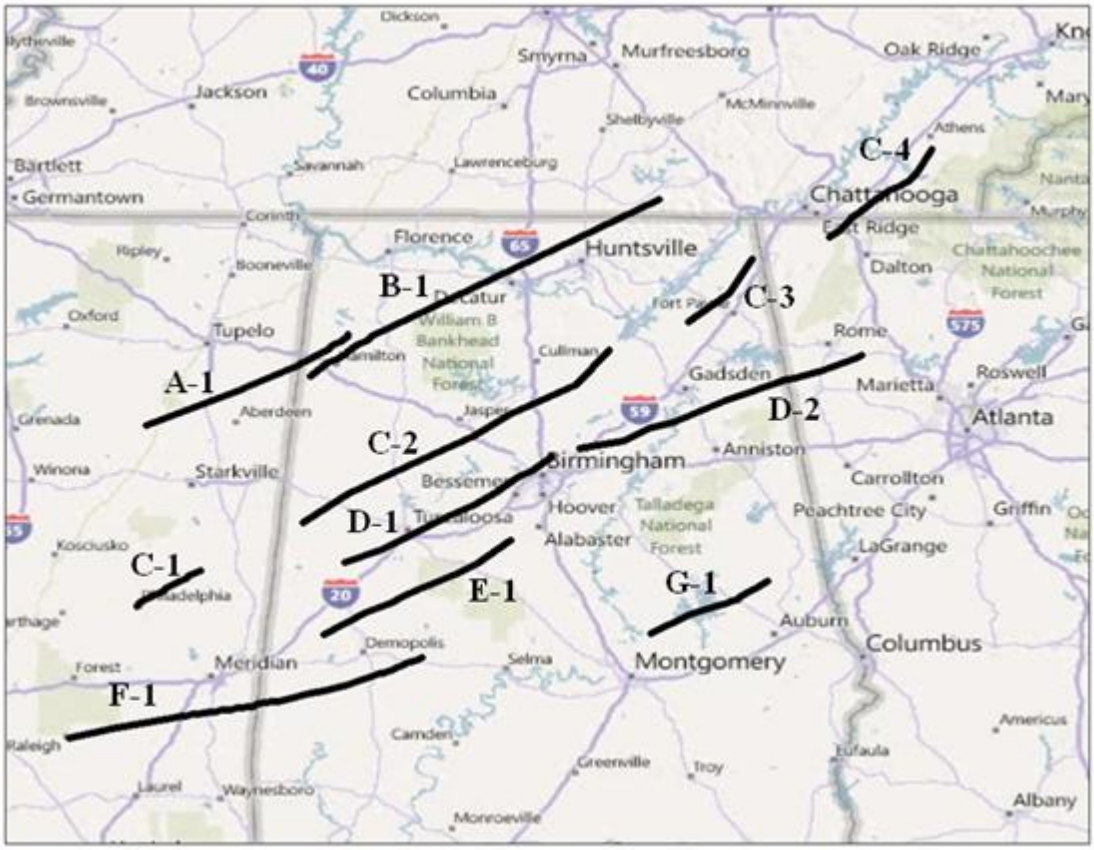

Figure 1: Paths of the tornadoes produced by the seven supercells examined. The letters represent the storms that were responsible for producing the tornadoes and the numbers represent the sequential order of the tornadoes produced by a particular storm throughout the severe weather event. (Ex. C-2 was the path of a tornado produced by Storm C and was the second tornado examined for supercell C within the research domain; cf. Table 1).

Table 2: Summary lightning metrics from the 300 km regional buffer centered on Birmingham, AL (19 UTC 27 April 27 2011 through 02 UTC April 28 2011).

Total CG lightning flashes	109,206
Total +CG flashes	5,889
Total -CG flashes	103,317
Percentage +CG flashes	5.39%
Average +CG flash polarity	24.13
Average -CG flash polarity	-19.82

Table 3: Lightning metrics for storms assessed (A-G) that fell within the 300km regional buffer on 27 April 2011 (19 UTC 27 April 27 2011 through 02 UTC April 28 2011)

Total CG lightning flashes	38,445
Total +CG flashes (kA)	2,528
Total -CG flashes(kA)	35,917
Mean max. +CG stroke current (kA)	39.96
Mean max. -CG stroke current (kA)	-85.49
Percentage +CG flashes (%)	7.45
Mean average -CG flash polarity (kA)	-21.54
Mean average +CG flash polarity (kA)	24.22
Avg. total CG flash rate (flashes min^{-1})	27.97

Table 4: Lightning metrics for the lifecycles of each storm (A-G) examined.

Storm	**A**	**B**	**C**	**D**	**E**	**F**	**G**
Total CG lightning flashes	1550	10084	7860	10496	2947	2315	3193
Total +CG flashes (kA)	93	780	434	598	237	183	203
Total -CG flashes (kA)	1457	9303	7425	9898	2710	2132	2990
Mean max. +CG stroke current (kA)	48.80	42.88	36.12	46.41	34.70	31.52	39.35
Mean max. -CG stroke current (kA)	-59.65	-78.69	-71.84	-106.6	-106.5	-80.44	-94.77
Percentage +CG flashes (%)	6.13	10.86	5.37	5.55	10.66	7.37	6.25
Mean average -CG flash pol. (kA)	-19.73	-19.16	-19.43	-20.79	-23.86	-24.48	-23.36
Mean average +CG flash pol. (kA)	32.16	21.72	23.25	23.04	22.00	22.94	24.48
Avg. total CG flash rate (flash/min)	14.17	59.65	21.12	45.69	16.09	11.16	27.97

Table 5: Lightning trends and attributes associated with each storm (A-G) ('✓' indicates experienced and 'X' indicates not experienced).

Storm	Tornado	Local max. total CG flash rate prior to tornadogenesis	Local min. total CG flash rate coincident with tornadogenesis	Polarity shift coinciding with tornadogenesis or during tornado production	Increase in total CG flash rate coincident with tornado dissipation
A	A-1	✓	X	X	X
B	B-1	✓	✓	X	X
C	C-1	✓	✓	X	✓
	C-2	✓	✓	X	✓
	C-3	✓	✓	X	✓
	C-4	✓	✓	X	✓
D	D-1	✓	✓	X	✓
	D-2	X	X	X	X
E	E-1	✓	✓	X	X
F	F-1	✓	✓	X	✓
G	G-1	✓	✓	X	✓

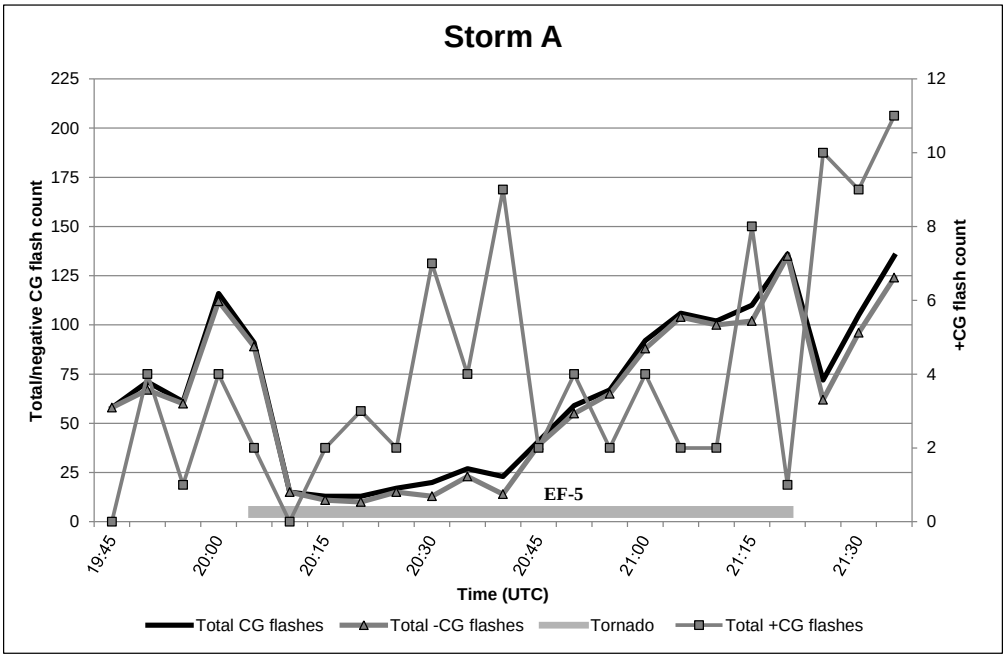

Figure 2: Temporal lightning trend analysis throughout the lifecycle of Storm A Thick black line indicates total CG flashes; gray line with the triangle marker illustrates total -CG flashes; gray line with the square marker represents the total +CG flashes; thick gray line with no marker represents the duration of the tornado.

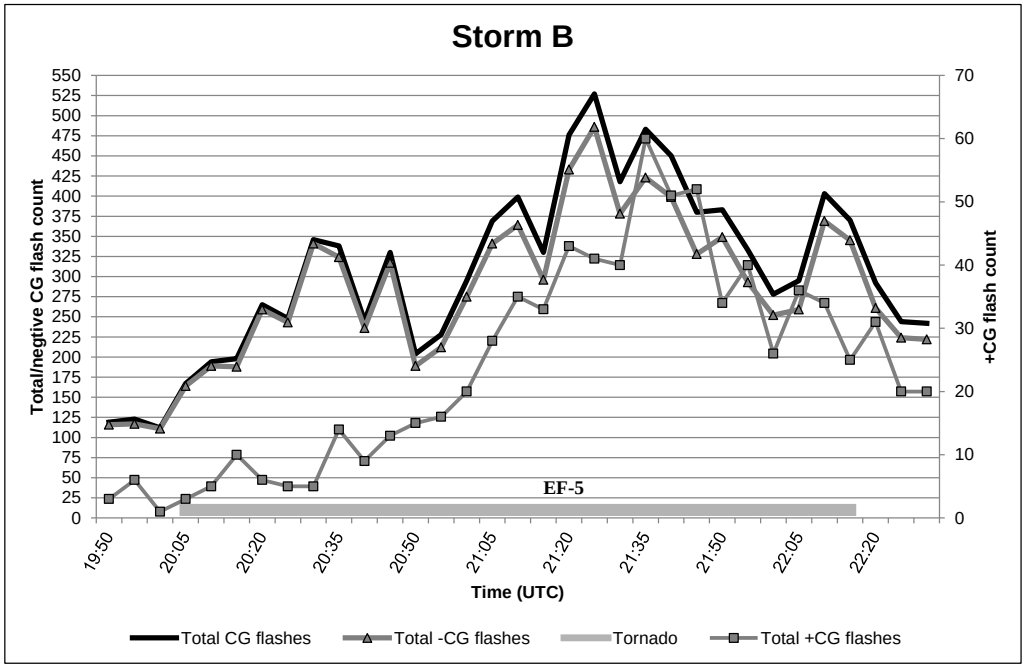

Figure 3: Same as Figure 2, except for Storm B.

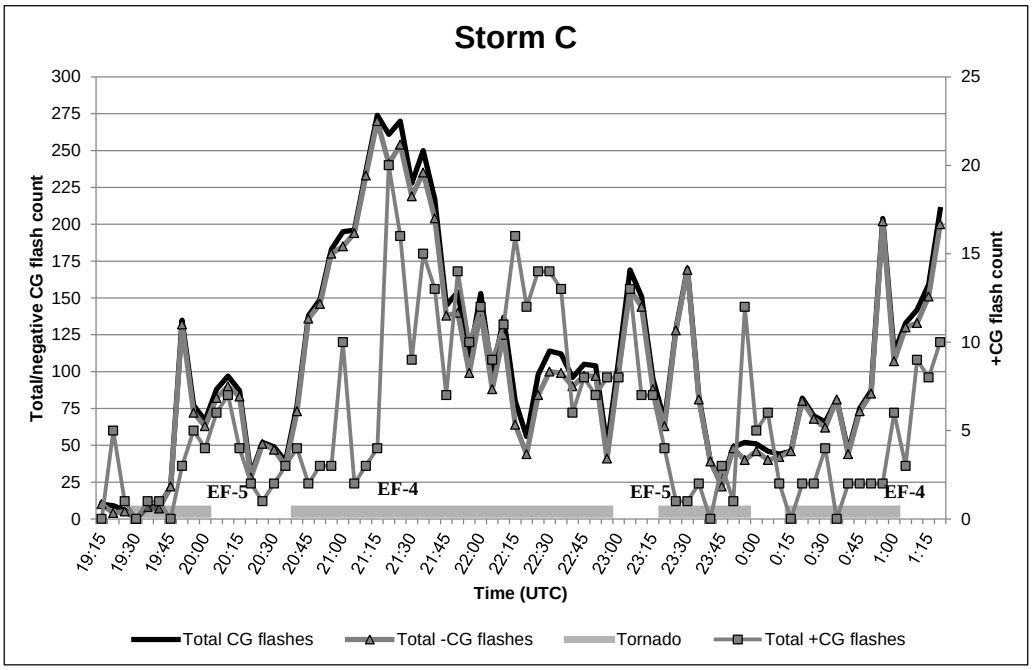

Figure 4: Same as Figure 2, except for Storm C.

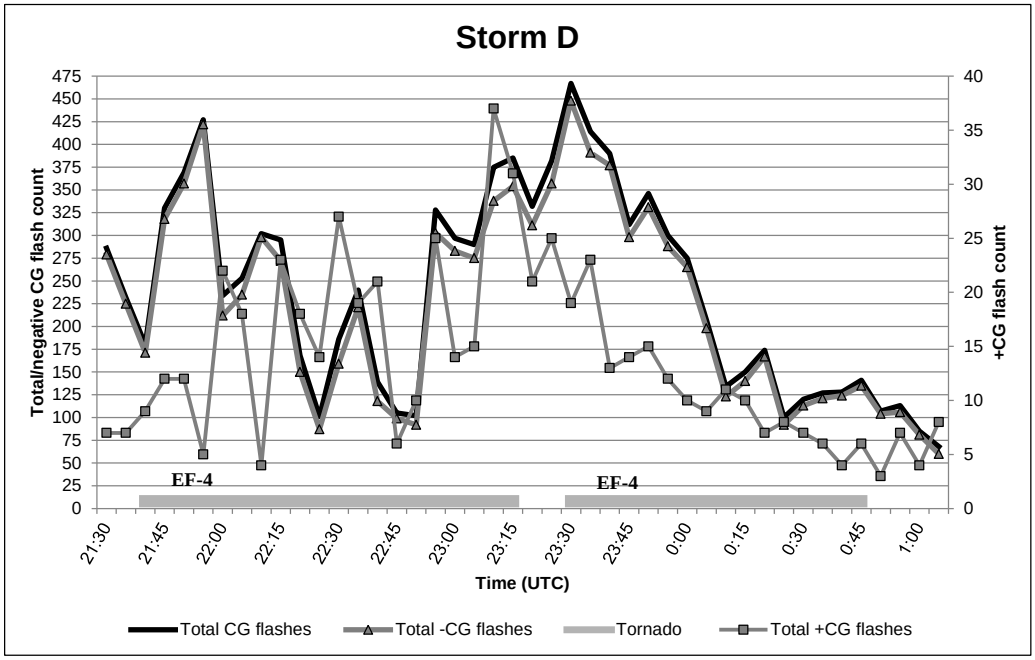

Figure 5: Same as Figure 2, except for Storm D.

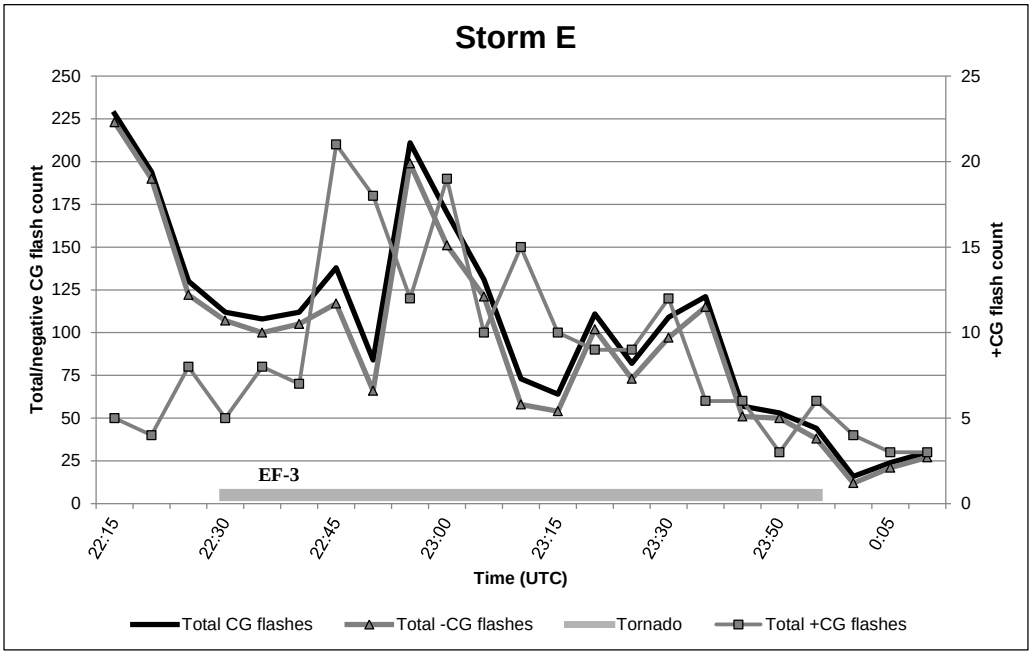

Figure 6: Same as Figure 2, except for Storm E.

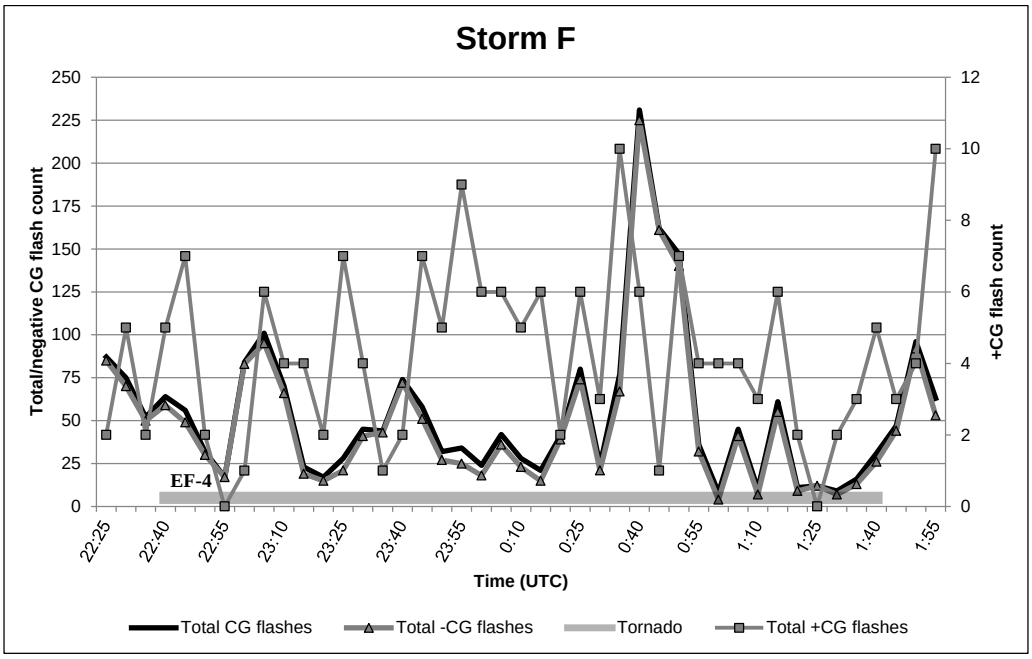

Figure 7: Same as Figure 2, except for Storm F.

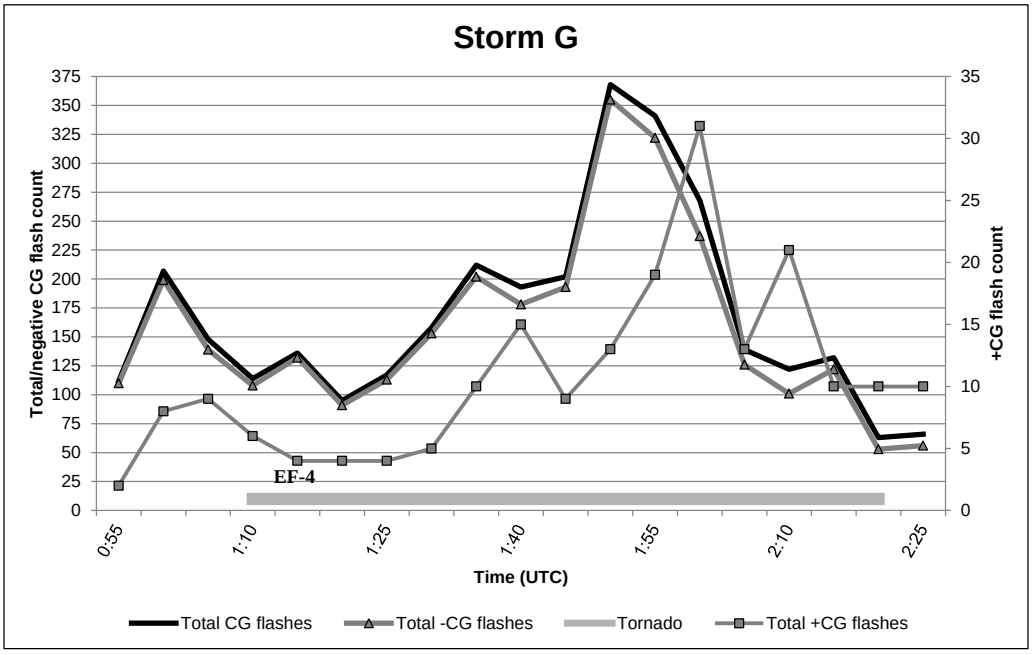

Figure 8: Same as Figure 2, except for Storm G.

Table 6: Storm D/tornado D-2 regression analysis (R^2), Pearson's product-moment correlation (r), significance testing with the t-distribution between total CG lightning flashes and rotational velocity (Vr)/azimuthal (rotational) shear (S) by Doppler radar scan elevation angle; values in bold font represent *moderate* correlation strength; values italicized illustrate significant correlation values.

	Vr (.5)	Vr (.9)	Vr (1.4)	S (.5)	S (.9)	S (1.4)
R^2	0.240	0.234	0.425	0.035	0.062	0.120
r	**-0.489**	**-0.483**	**-0.652**	-0.186	-0.249	**-0.346**
Significance test with the t-distribution One-tailed; α= 0.05	*-3.125*	*-2.974*	*-4.787*	-1.054	-1.382	*-2.052*

Table 7: Same as Table 6, except for Storm E/tornado E-1.

	Vr (.5)	Vr (.9)	Vr (1.4)	S (.5)	S (.9)	S (1.4)
R^2	0.052	0.039	0.003	0.037	0.257	0.004
r	0.228	-0.198	0.053	-0.192	**-0.507**	-0.064
Significance test with the t-distribution One-tailed; α= 0.05	0.968	-0.834	0.184	-0.805	*-2.427*	-0.224

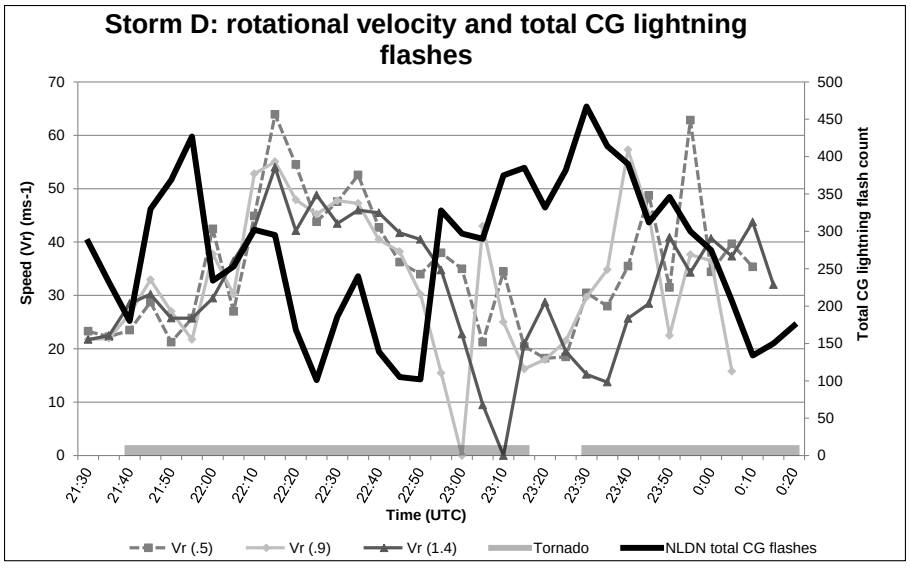

Figure 9: Storm D/tornadoes D-1/D-2 rotational velocity (Vr) and total CG lightning flashes via the NLDN; Solid black line represents the total CG flashes; darker gray line with the square marker illustrates the rotational velocity at radar elevation angle 0.5°; light gray line with the diamond marker indicates the rotational velocity at radar elevation angle 0.9°; gray line with the triangle marker represents the rotational velocity at radar elevation angle 1.3°.

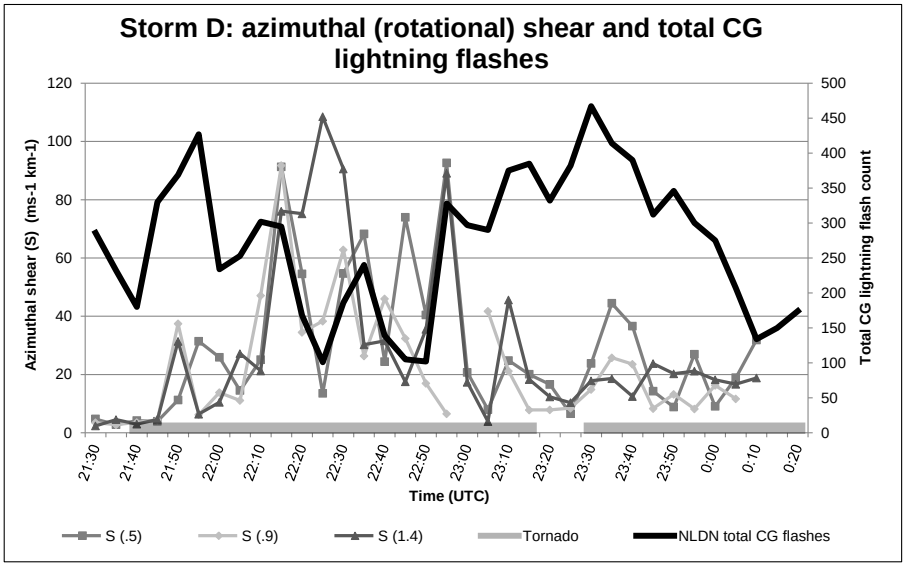

Figure 10: Storm D/tornadoes D-1/D-2 azimuthal (rotational) shear (S) and total CG lightning flashes via the NLDN. The solid black line represents the total CG flashes; the darker gray line with the square marker illustrates the azimuthal shear at radar elevation angle 0.5°; the light gray line with the diamond marker indicates the azimuthal shear at radar elevation angle 0.9°; the gray line with the triangle marker represents the azimuthal shear at radar elevation angle 1.4°.

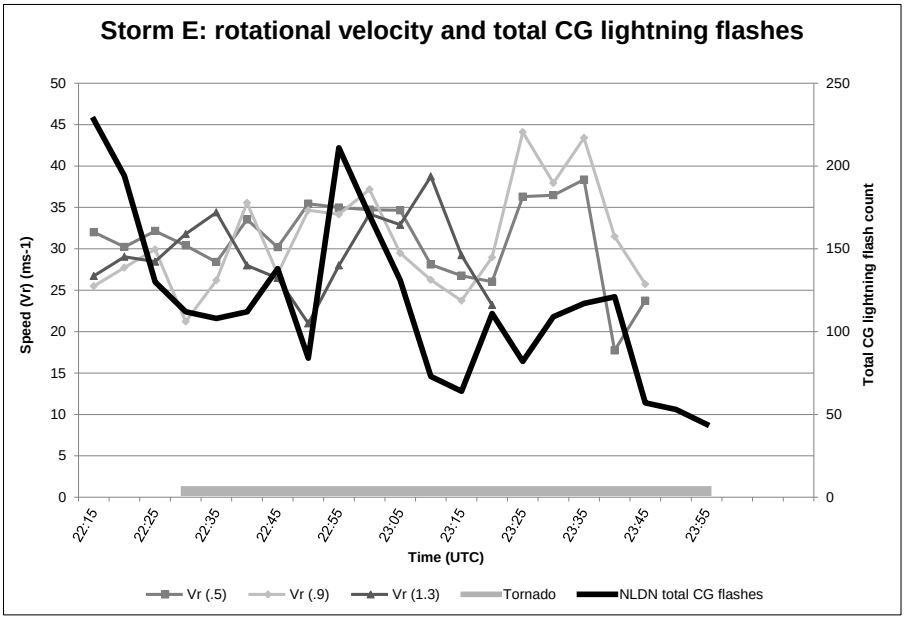

Figure 11: Same as Figure 9, except for Storm E/tornado E-1.

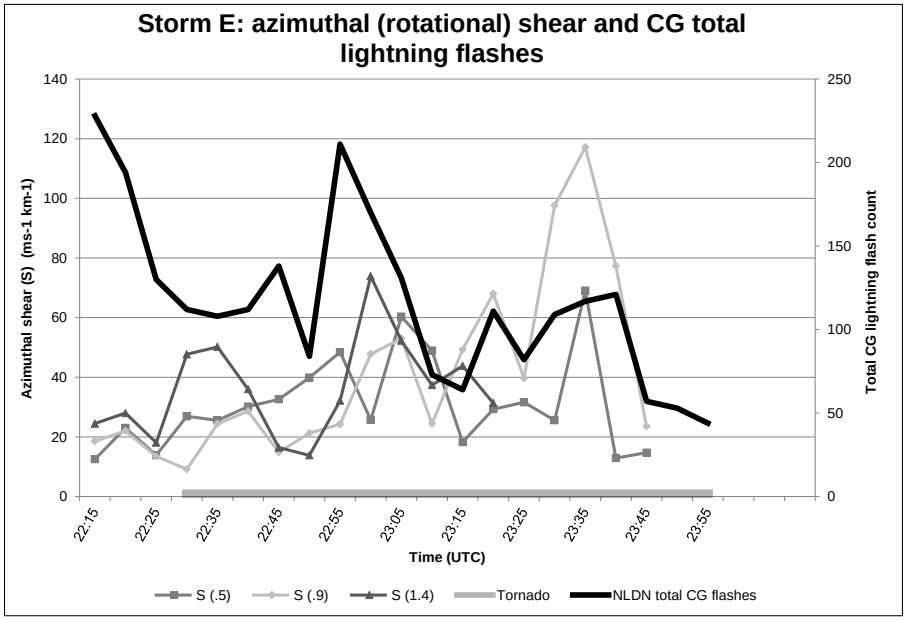

Figure 12: Same as Figure 10, except for Storm E/tornado E-1.

Table 8: Same as Table 6, except for Storm C/tornado C-2

	Vr (.5)	Vr (.9)	Vr (1.4)	S (.5)	S (.9)	S (1.4)
R^2	0.404	0.394	0.436	0.102	0.094	0.120
r	0.635	0.628	0.660	0.320	0.307	0.346
Significance test with the t-distribution One-tailed; α= 0.05	4.275	4.270	4.570	1.752	1.706	1.952